

# Kirim Pak Andri/573 Check.docx

# Design and kinematic analysis of a two-DOF moving platform as a base for a car simulator

---

## Abstract

The study starts by modeling a simple 2-DOF (degrees of freedom) moving platform that employs two actuators to provide two kinds of rotational motion on the moving platform and each motion is driven by an electrical motor. A preliminary study to better understand motion generation is conducted by deriving a mathematical model of the platform. Based on this model, the relationship between the rotations of the two driving motors and the pitch and roll movements of the platform is determined. The range of movements must be limited both in the pitch and roll planes to a certain maximum and minimum values of tilting angles. This preliminary design of the platform is introduced to demonstrate motions that might be experienced by the user in roll and pitch directions. The motion generated has fulfilled the constraint with respect to the vestibular system. Results of experimental works show that the first motor angle between  $-26^{\circ}$  and  $27^{\circ}$  is suitable for the roll plane; meanwhile, the angles range of  $-52^{\circ}$  and  $54^{\circ}$  for the second motor is suitable for the pitch plane. Furthermore, some simple experiments were conducted to examine the correctness of the model through the comparison between testing results obtained from simulation and experimental work. In the reported results, the moving platform was set to some initial poses and was driven to the home position and the recording showed acceptable results. This moving platform can later be used for more comprehensive experiments, i.e., vehicle dynamic testing, driving training purposes, and human factor analyses.

Keywords: human vestibular system; kinematic model; moving platform; pitch and roll planes; rotating encoder.

---

## I. Introduction

In recent years, advanced simulators are already well known in the field of computer science and engineering, as they are supported mainly by advanced computer technology development and thus are now significantly becoming indispensable in most engineering areas. The design and the use of simulation applications offer some benefits which can be obtained for obvious reasons, such as from flexibility, safety, and cost reduction points of view. In a simulation environment, the actors can try many aspects of the activity that must be researched or evaluated safely without worrying about dangerous things,

as if these activities were performed directly in the real situation.

Along with the development of technology, a technology called mobile platforms or motion platforms for driving simulators emerged. A mobile platform is a tool that has a mechanism to simulate the translational and rotational movements of the user. This mobile platform structure can be used to simulate the vehicle motion and the dynamics such as shocks or vibrations and maneuvers in-car simulation. It has several different purposes, such as driver training, simulation of mitigation activities, research on driver behavior, car safety evaluation and emergency system, and even for some entertainment facilities. Furthermore,

this driving simulator must be equipped with several important information/signals so that the driver does not lose his sense of reality when controlling a car as in real driving situations.

In addition to simulating vehicle movements, this motion platform can be used to complement racing games with hardware that provides a real driving experience. The simulator can further be used to simulate driver/pilot training purposes and experiences done by Brookhuis in [1], for human factor analysis by Kuiper et al. in [2], for evacuation simulations in the case of a tsunami by Maruyama and Sakaki in [3] as well as for evaluating the visual interface experiments of in-vehicle information system for elderly by Gomez et al. [4].

Simulators have been accepted widely by many researchers because they have made research activities easier. They can keep users away from the possibility of accidents or unwanted events. Meanwhile, Maruyama and Sakaki [3] proposed a driving simulator for evacuation experiments in the case of a tsunami. This study developed a system equipped with 3D computer graphics installed in the driving simulator. The system consists of three LCDs, a steering wheel, a brake, and acceleration pedals. An experiment was conducted with ten participants. The visual information about tsunami was close to reality and gave a better insight of the disaster without having to be physically in an unwanted situation.

Through this simulator platform development, Gomez et al. [4] allowed the users to modify the configuration openly and flexibly, reconfigure and evaluate prototypes of safety and emergency systems, apply a variety of driving scenarios, and so on. Users may also have the possibility to adapt with user-dedicated facilities, i.e., hardware and/or software when developing or evaluating new systems. Two examples of the application of the driving simulator platform are presented, which may contribute to improve road safety.

Based on research by Berthoz et al. [5], car simulators equipped with motion cues could provide a more realistic driving experience for users. In the experiment research, users with a car simulator that has a movement output can complete a slalom test simulation better than a simulator that does not have a movement output.

The movement specifications of the moving platform should also be adapted to the human sense of balance. The human sense of balance is the vestibular system (vestibular nerve), and this system is located in the human inner ear. The vestibular system can detect the

orientation of the head and the direction of the earth's gravity concerning the body [6]. Both of this information is needed by the brain to maintain balance and body orientation while moving. Meanwhile, Hansson et al. [7] mentioned that tilting the cabin of a simulator platform gives rise to a perceived linear acceleration, which would not happen in reality. The practice called tilt coordination (TC) in combination with visual cues may be perceived as continuous linear acceleration. This must be considered in platform operations to avoid presenting false cues, motion sickness, and other negative effects.

According to Bringoux et al. [8], the limit of the vestibular system for sensing tilt (roll and pitch) is  $6^\circ$ . This figure determines the maximum allowable range of rotational motion of the moving platform. Moreover, according to Stratulat et al. [9], the limit of the vestibular system for sensing radial velocity is 3.7 deg/s. However, based on research by Groen and Bles [10], the movement of the car simulator will be more realistic when the entire car simulator platform is tilted with a radial speed that does not exceed 3 deg/s. Most articles cited above did not explore the mechanical structure in detail and what other factors were concerned when developing the corresponding moving platform.

Mostly manufactured motion-simulator platforms are actuated using more than 3 actuators, such as in [11][12], and in some cases by using 6 actuators, such as the Stewart platform [13]. Some designs allowed translation effects that were introduced by Arioui et al. [14] and even used a complicated cabling system to reach a very easy moving platform [15]. This makes the designs not simple to implement and manufacture.

The only motion structure that is quite similar to this design is the one shown by Alsina et al. in [16], where their mechanical platform is used as a motion generator that emulates pitch and roll movements typically measured along the Catalan coast, but no mathematical formulations were derived. Some other structures present the same (similar) ideas to produce a  $2^\circ$  motion using two actuators are shown by Ahmad et al. in [17] and by Bin Mohd. Nadiman in [18]. They all use a single supporting point almost in the lower-middle part of the platform as the pivot point. The existence of this pivot provides easy rotation around the x-axis (rolling) and y-axis (pitching), but this prevents the structure from having translational motion in any direction. As a consequence, these designs will not match if the future development is going to allow translational motions.

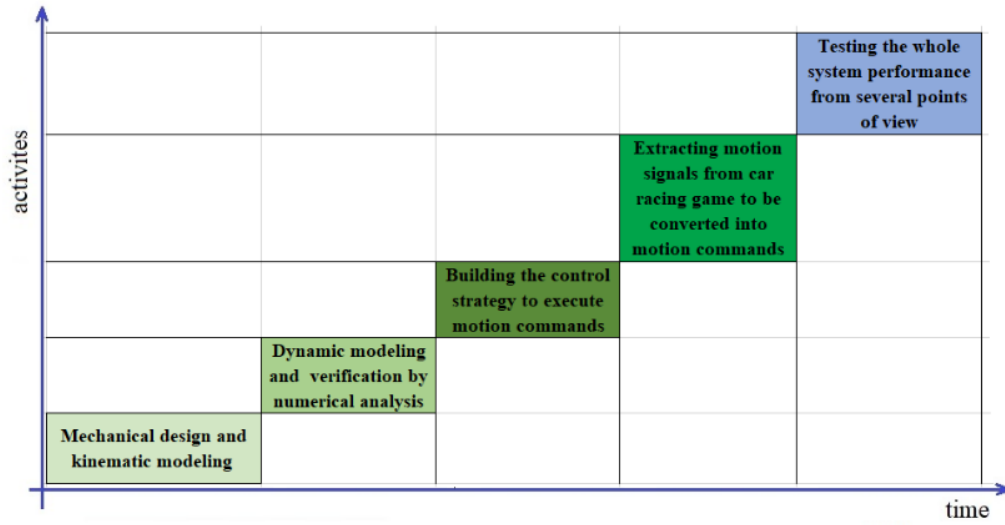


Figure 1. Five research stages in developing the complete moving platform

As a mechatronic engineering school, we believe that the project of making a fully computerized controllable car simulator is a very suitable topic to show how mechatronics is involved in this kind of activity, starting from determining the user specifications and constraints, mechanical structure and mechanism, electronic and power, dynamics, and control, and finally evaluating the overall performance. Mechatronics students or researchers with diverse backgrounds in the field of mechatronics can contribute, collaborate, and synergize themselves to find the most suitable solution.

In general, the research question to be analyzed is what kind of platform is appropriate as a base for car simulation that can properly respond to any command to the actuators and can show the behavior of the moving-simulator platform. Then the aim/objective is to make a platform capable of rotating in both roll and pitch planes and complying with the constraint of the vestibular boundary mechanism. In this study, a concept in which a car simulator platform, such as those used in a racing game simulation, is developed. Its basic features are evaluated, i.e., the range of rotation, the limit of rotation, motor speed, etc.

## II. Materials and Methods

The existing simulators mostly are fully controllable for performing the 6-

DOF (degrees of freedom) motion; therefore, the structures are most complicated. To begin with, a 2-DOF moving platform is introduced. The model is discussed only from a kinematic point of view. The stages in developing this moving platform are shown in Figure 1. Firstly, the kinematic model of the platform and testing is developed. Second, the dynamic mathematical model is derived and verified by numerical analysis. Third, the control strategy to execute the motion commands is built. Fourth, motion signals from a car racing game are extracted to be converted into motion commands. Finally, the whole performance of this moving platform as a complete car simulator is tested from different points of view, even the evaluation of the vestibular boundary criteria.

In the early stage of development reported in this study, the kinematic model of the moving platform is constructed, the mathematical model that relates the platform orientation (tilting angle) and actuating angle is calculated, and then some simple motion tests were conducted to verify the correctness of the model. A simple electronic circuit operates to measure the platform orientation and executes the desired actuator rotation angles.

### A. Kinematic model development of the platform

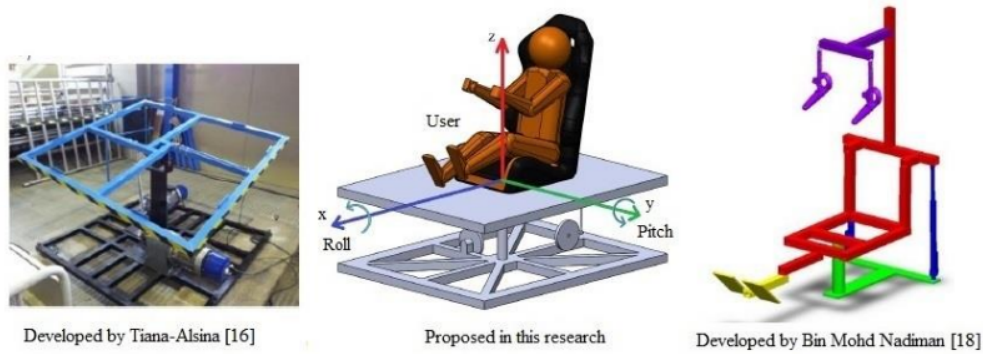


Figure 3. Three similar designs to produce rolling and pitching rotation

The moving platform, designed as a car simulator, has 2-DOF, namely motions in roll and pitch directions. Firstly, the model was designed on SolidWorks software, where the platform is supported in the center and two actuators are positioned underneath to perform actuation. The support is one pivot joint in the lower middle of the platform base. Two DC motors are employed at two certain distances perpendicular to each other from the pivot to actuate the platform in two planes, each responsible for actuating 1-DOF motion. Two sets of serial links perform a slider-crank-like mechanism (connecting rod and crank in the form of a circular plate) to move the platform up and down. The 3D model of the proposed platform and its real structure, which is manufactured from a hollow steel bar, is shown in Figure 2.

To anticipate the free (3D) movement of the connecting rod between the motor disk and actuating point at the platform, a universal joint is introduced. The mechanism is arranged perpendicular to each other. This design aims to make the structure as simple as possible using only two actuators but is capable of showing the motions of a car simulator. Furthermore, this design makes manufacturing easy and simplifies system analysis.

The platform dimension has a length of 1500 mm and a width of 1200 mm;

meanwhile, the free space between the platform and base is 400 mm. Since the moving platform is analyzed as a two planes case, then the two planes are defined as follows:

- The pitch plane is the x-z plane used to analyze the movement of the platform when tilting forward and backward (pitch rotation)
- The roll plane is the y-z plane used to analyze the movement of the platform when tilting to the left and the right (roll rotation)

Platform motion in both planes will be defined completely in the same mathematical formulation, but the difference is only in the physical dimensions (values) of all corresponding variables. This makes the reader easier to understand the working of the mechanism.

As mentioned earlier, there are two designs very similar to the one proposed in this article, i.e., the one by Tiana-Alsina et al. [16] and the other by Nadiman [18]. The 3D model comparison of those three designs is depicted in Figure 3. It is shown that the pivoted support in the lower middle of the platform prevents the translational motion in all directions from being happened. Among them, the way to actuate the platform of Nadiman [18] is the most complicated one, in which a combination of the motion of the two actuators will perform the roll and pitch motions.

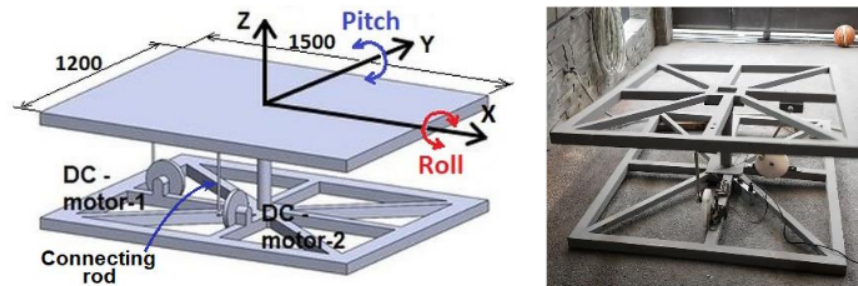


Figure 2. A 3D model of the moving platform and the manufacturing testbed

The position where the user/car driver sits when operating the platform is determined by calculating the center of gravity (COG) of the user's side view. The location of the center will influence the reaction of the motor to perform the motion. The coordinates of the user's COG can be determined using the area approximation of the blue and red areas, as shown in Figure 4. Because the used area is in a digital image, the unit used in calculating this COG is the pixel. The origin point located at the bottom left of the COG obtained from this approach is (861,845) pixels.

While capturing the picture, the user holds a scalable ruler. The maximum length will later be associated with the number of pixels measured for the ruler. From the picture examination, it is seen that 300 mm corresponds to 533 pixels. Because the coordinates of the obtained COG are still in pixels, these coordinates need to be converted into millimeters. These coordinates are converted using a multiplying factor  $k_z$ , as defined in (1). The  $k_z$  factor is obtained as follows:

$$k_z = \frac{300}{533} \text{ mm/p} \quad (1)$$

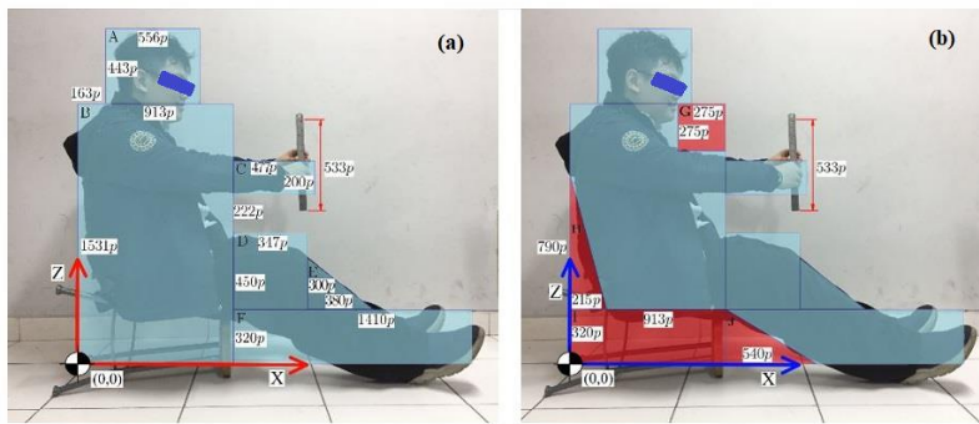


Figure 4. Simplified body form of the user for calculating COG



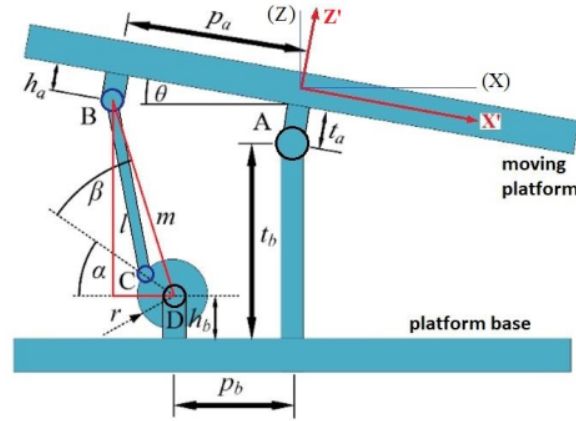


Figure 5. Side view of the platform

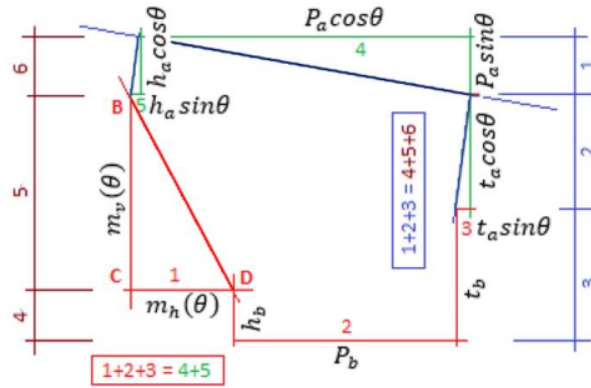


Figure 6. Relation of dimension variable

The calculated COG of the user on the x-z plane is (484,476) mm and is measured from the origin point. This figure will be mainly used in the dynamic analysis of the system (which will be examined in the next stage of the research, as mentioned earlier). The COG of the user in y-z is in the center plane.

### B. Mathematical model of the motion platform

The relationship between moving platform orientation and the rotation angle of the DC motor is the main concern in the mathematical formulation. In Figure 5, all variables related to the physical dimension of the platform are defined. The radius (CD) of crank (wheel) is defined as  $r$  and the length of connecting rod (BC) is defined as  $l$ . Meanwhile, a more specific relationship between them is defined, especially in relating the motor ( $\alpha$ ) and the platform tilting ( $\theta$ ) angles in Figure 6.

The equation of the relationship between the motor rotation and the platform orientation is first derived based on kinematic relation. It is later used to simulate the movement of the moving platform. To define this

relationship, the platform kinematic structure in Figure 2 is simplified into simpler variable relations, as shown in Figure 6.

The red triangle (BCD) in Figure 6 is analyzed to get the relationship between the platform and the motor angle ( $\theta$  and  $\alpha$ ). The height of the triangle is defined as  $m_v$ , the length of the base is defined as  $m_h$ , and the length of the hypotenuse is defined as  $m$ . Their definition is a function of angle  $\theta$  are shown in (2), (3), and (4):

$$m_h(\theta) = p_a \cos \theta - p_b + (h_a - t_a) \sin \theta \quad (2)$$

$$m_v(\theta) = p_a \sin \theta + t_b - h_b + (t_a - h_a) \cos \theta \quad (3)$$

$$m(\theta) = \sqrt{m_v^2(\theta) + m_h^2(\theta)} \quad (4)$$

Using the cosine rule, the angle  $\theta$  is calculated in (5) or (6) as follows:

$$\cos[\alpha(\theta) + \beta(\theta)] = \frac{m_h^2(\theta) + m^2(\theta) - m_v^2(\theta)}{2m_h(\theta)m(\theta)} \quad (5)$$

$$\alpha(\theta) = \cos^{-1} \left[ \frac{m_h^2(\theta) + m^2(\theta) - m_v^2(\theta)}{2m_h(\theta)m(\theta)} \right] - \beta(\theta) \quad (6)$$

The measurement of the angle  $\beta$  is calculated using the following cosine rule:

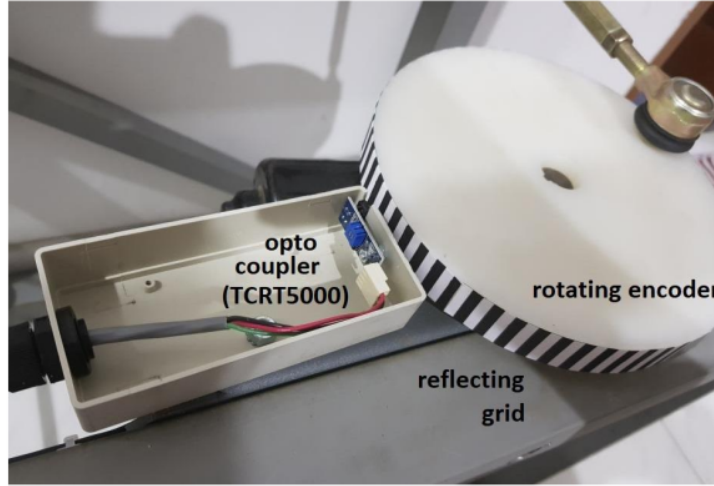


Figure 7. Rotating encoder and its mounting

$$\cos \beta(\theta) = \frac{r^2 + m^2(\theta) - l^2}{2rm(\theta)} \quad (7)$$

$$\beta(\theta) = \cos^{-1} \left[ \frac{r^2 + m^2(\theta) - l^2}{2rm(\theta)} \right] \quad (8)$$

The relationship between the motor angle and the platform angle  $\theta$  is obtained by substituting (8) into (6).

$$\alpha(\theta) = \cos^{-1} \left[ \frac{m_h^2(\theta) + m^2(\theta) - m_v^2(\theta)}{2m_h(\theta)m(\theta)} \right] - \cos^{-1} \left[ \frac{r^2 + m^2(\theta) - l^2}{2rm(\theta)} \right] \quad (9)$$

Eventually, (9) can be used to analyze moving platform motion in roll and pitch plane by using inputs in the form of incremental values of the corresponding variables.

#### C. Simulation of the motion platform

As mentioned earlier, (9) is used to simulate the motion of the platform using MATLAB software. The variable magnitudes used in this equation are  $l = 320$  mm,  $r = 75$  mm,  $h_a = 30$  mm,  $h_b = 50$  mm,  $t_a = 50$  mm, and  $t_b = 350$  mm.

When analyzing the pitch plane, the variable values are  $p_a = 575$  mm and  $p_b = 500$  mm. In the roll plane, the variable values are  $p_a = 325$  mm and  $p_b = 250$  mm.  $p_a$  and  $p_b$  values were obtained from the best value of an iteration process, which gives a tilting angle on roll and pitch planes between  $-6^\circ$  to  $6^\circ$ . This search was done by trial and error.

The simulation was carried out by correlating tilting angle  $\theta$  with actuating angle ( $\alpha$ ) ranging from  $-100^\circ$  to  $80^\circ$  for both roll and pitch planes. An increment of  $0.1^\circ$  for angle ( $\theta$ ) is fed to (9) and the corresponding angle ( $\alpha$ ) is recorded. After running the simulation, the relation between tilting angle ( $\theta$ ) and actuating angle ( $\alpha$ ) can be obtained.

#### D. Platform testing methods

The process of testing the platform is done by actuating the DC motor within the angle range provided by the simulation. In this stage, the platform tilting angle is measured using the MPU6050 module mounted on the platform, which is capable of measuring velocity, orientation, acceleration, displacement, and other motion-like features. The MPU6050 sensor is used to detect the platform tilting angle directly. Meanwhile, Saputra et al. [19] introduced a comprehensive explanation of using inertial measurement unit (IMU) to calculate absolute and relative attitudes for controlling joint angles of a pan-tilt mechanism. Rafiq et al. [20] used the same MPU6050 module to detect the tilting angles in the development of the smartphone gimbal. Zhang et al. [21] showed the implementation of IMU for outdoor applications where estimation of absolute attitude is compared with a kinematic model of motion, while Albaghdadi and Ali [22] introduced detailed methods to overcome measurement error caused by vibration when using the MPU6050 module. Jefiza et al. [23] and Al-Dahan et al. [24] used the MPU6050 module to detect the fall of the elderly when walking, while Rifajar and Fadlil [25] used it to detect the fall of a dancing robot by monitoring the acceleration of rotational motion. The approach to measuring joint angles in this research is different, where the measured orientation is used to calculate joint angles of the DC actuators based on (9).

The TCRT5000 sensor (rotating encoder) is placed in front of the segmented grid of the circular plate (motor disk), as shown in Figure 7. The encoder (TCRT 5000 sensor) is used to detect the motor



angle by counting the number of black-white grids that pass in front of the optocoupler. For one complete rotation of the rotating disk, 65 black grids correspond to  $5.54^\circ$  reading accuracy. This is a good example of the implementation of a low-cost self-made rotating drum encoder for mechatronics or other engineering students.

### III. Results and Discussions

#### A. Kinematic model of the platform

From Figure 2, one can see clearly a very rigid structure of the moving platform and the dimension is big enough for a person who will drive the platform. It is easy to model the platform in SolidWorks by utilizing the 3D solid model to make the platform. Having done the 3D model, dimensions and all connections between frames are used as a reference to manufacturing the platform. The material used is a hollow steel bar and the connection between frames is done by welding.

The slider-crank-like mechanism converts the motor rotation into a vertical translation motion at the connecting pin at the platform. Two vertical thick plastic disks acting as the crank arms are mounted between DC motor axes and the connecting rod. In the end, this motion generates the rolling and the pitching motion in their respective planes. This mechanism is the realization of a four-linkage mechanism, where the rotation of the first link is directly followed and converted by the third link. Because of the physical dimensions, the magnitude of the tilting angle on each plane (roll and pitch) differs, directly determining the working range of each driving motor.

As the platform is actuated by two actuators  $90^\circ$  from each other, this mechanism works not always in a fixed plane but always in a free-oriented

plane. To deal with this condition, a universal joint has to be implemented to accommodate the connection of a rigid bar between the free-oriented plane and a fixed-oriented plane. This is a common mechanical engineering practice.

#### B. Mathematical model of the motion platform

A mathematical model is essential to find the exact correlation between the input signal (actuator motion) and output (platform tilting angles). For this motion platform, actuating angle as input corresponds directly to the platform tilting angles with respect to all physical parameters of the platform. Equation (9) has determined the relation between the tilting angle and the motor angle. The magnitude of these tilting angles depends directly on the base distance of the actuator ( $p_b$ ), the linear distance of the pivot ( $p_a$ ), and the length of connecting rod ( $l$ ).

Because the tilting angle of the platform must be limited due to the vestibular boundary conditions, the actuating angle ( $\alpha$ ) is restricted as well. The range of actuating angles for generating roll motion is  $-26^\circ$  to  $27^\circ$ , and for generating roll motion is  $-52^\circ$  to  $54^\circ$  (Figure 8). This angle will determine the length of a moment arm, which later directly defines the magnitude of the motor torque required. One can understand the smaller the angle range, the smaller the torque required. The angle ranges in this design are good as the longest moment arm exists when the motor angle is  $90^\circ$ . It can be clearly understood based on statics analysis in engineering mechanics.

#### C. Motion command system of the platform

The platform motion is controlled by an Arduino UNO microcontroller and the DC motors are driven by a 12 V power supply. To control the motor speed and

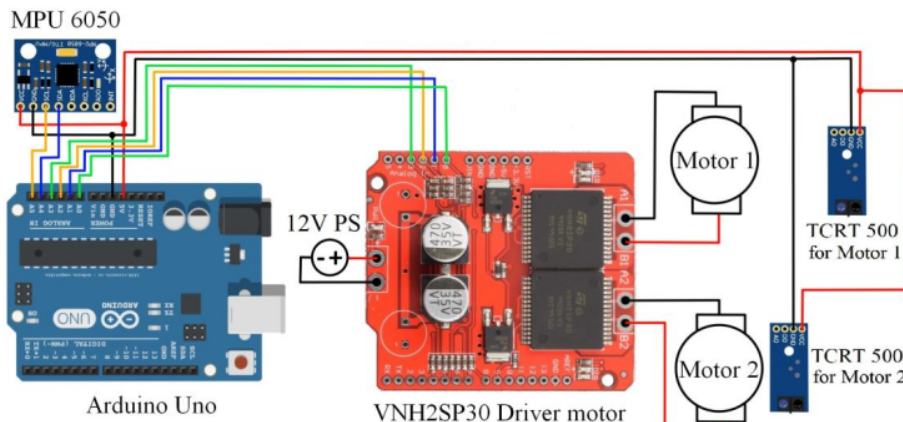


Figure 8. Electronic circuit for controlling the DC motor

directions, Monster Moto Shield VNH2SP30 driver is employed. The driver is controlling the voltage polarity and magnitude to be sent to both motors based on the signal information from the Arduino. The circuitry for controlling the motors is depicted in Figure 8. Motor speed is set to 20% of maximum magnitude (in the range of integer numbers: 0 to 255) and there are some default commands to move CW, CCW, and BRAKE. A simple program coding is prepared to let a motor move in a certain direction at a certain speed. An example of the coding is as follows:

```
motorGo(MOTOR_1,CCW,55);
where MOTOR_1 means motor 1 is active,
CCW means motor rotation
(counterclockwise), and 55 means motor
speed (speed range of 0 to 255).
```

A simple if-then rule is used to command the motor moves to a certain position, such as:

```
If (in position within tolerance)
    motor stops
```

```
else if (position > target)
    run motor CW
```

```
else if (position < target)
    run motor CCW
```

All these codes are enough to command the motors to move in any position within the angle range values based on the simulation.

#### **D. Experimental results: accuracy and sensitivity of the platform**

The process of testing the platform is firstly done by performing simulation

separately between roll and pitch planes, wherein incremental angle input ( $\theta$ ) is fed to (9). The range of angle input ( $\theta$ ) is between  $-15^\circ$  to  $12.5^\circ$  for the roll plane and  $-8.5^\circ$  to  $6.9^\circ$  for the pitch plane. The function of angle ( $\theta$ ) in respect to angle ( $\alpha$ ) is plotted as depicted in Figure 9. The first simulation shows that the minimum tilting angle of  $-6^\circ$  was realized by  $-26^\circ$  and the maximum tilting angle of  $6^\circ$  was realized by  $27^\circ$  in the roll plane. The second shows that the minimum tilting angle of  $-6^\circ$  was realized by  $-52^\circ$  and the maximum angle tilting of  $6^\circ$  was realized by  $54^\circ$  in the pitch plane. Those numbers of actuating angles are now obtained and can be used as preliminary reference points.

The platform motion was examined for three cycles of execution, and both angles ( $\theta$  and  $\alpha$ ) were measured simultaneously. After then, the best result between  $-100^\circ$  to  $80^\circ$  rotation of actuating motor is displayed in Figure 10. The sensor reading ( $\alpha$ ) lies very close to the simulation result of the tilting angle ( $\theta$ ), then it proves that the mathematical model of the platform is correct or closely related to the measurement. From Figure 10, this range is delivered by two different motor rotations as the physical structure ( $p_a$ ,  $p_b$ , and  $l$ ) of each mechanism differs. This output range will become the maximum allowable output produced by both DC motors.

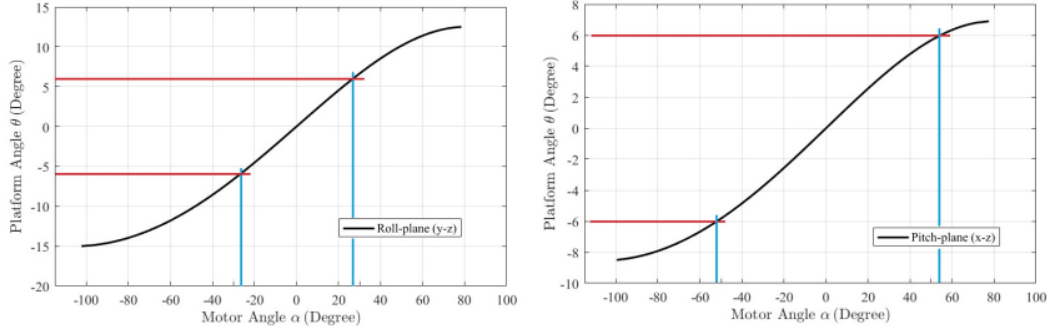


Figure 9. Simulation result of moving platform

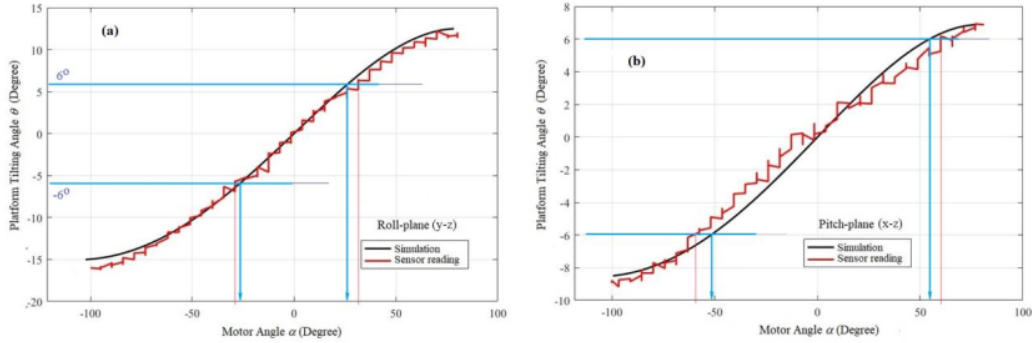


Figure 10. Comparison between platform tilting angle and motor angle in roll (left) and pitch (right) planes

The first experiment in Figure 10(a) shows that the minimum tilting angle of  $-6^\circ$  was realized by  $-30^\circ$  of actuation and the maximum tilting angle of  $6^\circ$  was realized by  $32^\circ$  of actuation in the roll plane. The second shows that the minimum tilting angle of  $-6^\circ$  was realized by  $-60^\circ$  of actuation and the maximum angle tilting of  $6^\circ$  of actuation was realized by  $61^\circ$  in the pitch plane. Figure 10 also shows that the range resulting from simulation can be considered a safe magnitude of actuator angles.

Another aspect used to show the discrepancy between the simulation and experimental result (Figure 10) is the comparison of areas under the span that corresponds to the platform angle range from  $-6^\circ$  to  $6^\circ$ . From the pitch plane, the area calculated from the simulation is 344.14 units and from the experiment is 331.32 units. So, we can roughly say that the error ( $e_p$ ) is:

$$e_p = \frac{344.14 - 331.32}{344.14} = 0.0373 = 3.73\% \quad (10)$$

From the roll plane, the area calculated from the simulation is 164.16 units and from the experiment is 172.78 units. So, we can roughly say that the error ( $e_r$ ) is:

$$e_r = \frac{172.78 - 164.16}{172.78} = 0.0499 = 4.99\% \quad (11)$$

The previously two error values suggested that the mathematical model of the platform conforms to the real physical structure. An error of less

than 5% is acceptable in the engineering field, and it can be minimized if not eliminated by the control algorithm designed for this purpose in future work.

Regarding the platform motion in the roll plane in Figure 10(a), the two graphics are in line very closely, while in the pitch plane in Figure 10(b), they lay apart from each other. It is logically understood as the sensitivity of motion in the roll plane is higher due to the base and supporting distances. There are still some discrepancies between the motor angle readings and angles recorded in the simulation when performing two directions of tilting. This is mainly caused by the inaccuracy of the rotating encoder used to measure the motor angle. We point out that a homemade encoder often shows inaccuracy in many cases.

Furthermore, some related experiments were also conducted, to show how the mechanism will bring the platform from one arbitrary pose to zero position. The results of these experiments are depicted in Figure 11.

There are four initial positions of the platform as detailed below:

- Roll plane at  $11.46^\circ$  and pitch plane at  $-4.81^\circ$
- Roll plane at  $-10.25^\circ$  and pitch plane at  $6.61^\circ$
- Roll plane at  $10.21^\circ$  and pitch plane at  $-6.58^\circ$
- Roll plane at  $11.49^\circ$  and pitch plane at  $5.96^\circ$

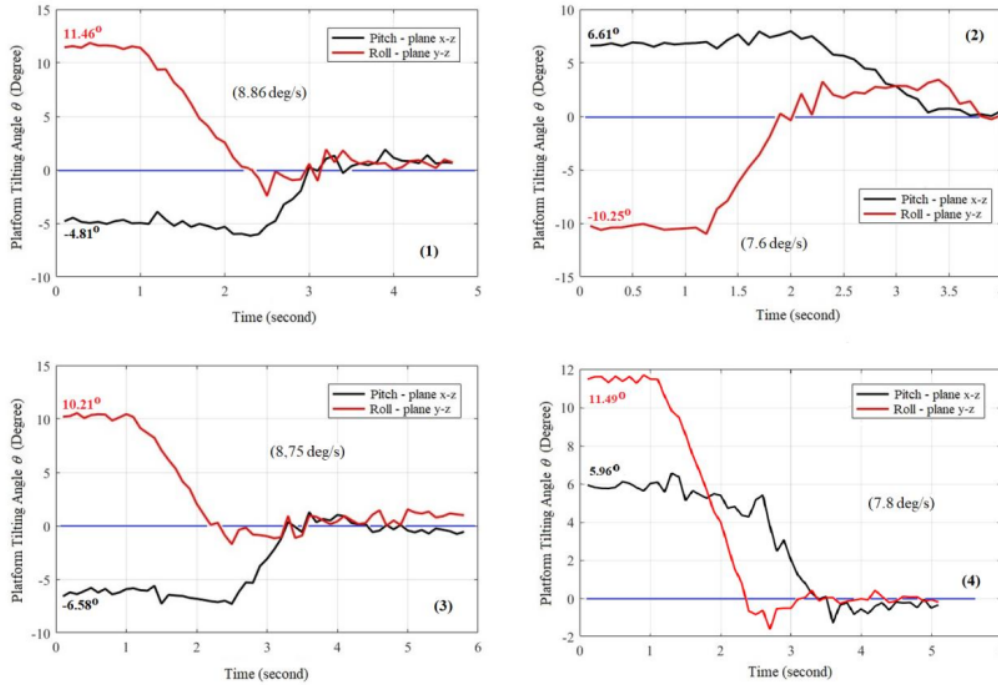


Figure 11. Four different starting poses to run to the home position

In the beginning, the zero position of the platform (upward orientation) is determined using spirit level both in the roll as well as in pitch planes. The output reading of the MPU6050 fluctuated between  $-0.67^\circ$  to  $0.68^\circ$  in the rolling plane and between  $-0.56^\circ$  to  $0.56^\circ$  in the pitch plane caused by the noise in the sensor electronics, which proves the existence of the sensing characteristic, that is, the floating phenomenon. Starting from four different poses, the motors gradually move to their home positions, respectively. The platform movement was established and completed at once, both in roll and pitch planes. The completion time of four executions was recorded as for 1) 3.4 s; 2) 3.8 s; 3) 3.6 s; and 4) 3.4 s, respectively. The maximum rotational speed of the platform achieved from all these experimental motions is 8.86 deg/s.

Other experiments were carried out to examine the motion of the platform moving to a certain desired orientation. The top two graphics in Figure 12 show the course of tilting angle from the home position to  $-10^\circ$  and then to  $8^\circ$  orientation in the roll planes. The bottom two graphic shows the course of tilting angle from the home position to  $6^\circ$  and then to  $-5^\circ$  in the pitch plane. The time-traveling shows a clear consistency that a bigger tilting angle requires a longer execution time. The maximum speed of the platform rotation achieved in all these tests is 20 deg/s.

The objective to make a platform having roll and pitch rotations has been

achieved and at once complying with the constraint related to the mechanism of vestibular boundary criteria. Comparing to other studies shown in [11][12][13], this study has much less capability and flexibility. Those cited works can change orientation in space while translating in any direction, but the models are much more complicated to analyze and implement. The objective of the design in this study is only to provide 2-DOF motion, i.e., roll and pitch rotations. The main advantage is a simpler design and mathematical analysis, cheaper alternatives, and easier use and maintenance.

Each platform direction may have a different speed due to its physical construction, meaning that each direction will have a different rotational speed. More attention must be paid as it is related to the boundary conditions of the vestibular system. For the same tilting angle (Figure 13), the rotational effect of the pitch will be much more significant, as the offset of COG position is small (Figure 13(a)) in the pitch plane compared to the rotational effect of roll (Figure 13(b)). This fact makes the pitching effect should be more pronounced for the user than the rolling effect. The illustration of those two cases is depicted in Figure 12.

The future work of this research is to develop the dynamic model of the moving platform. This model is important as the moving mass has a very big impact on the motion of the structure. Knowing the

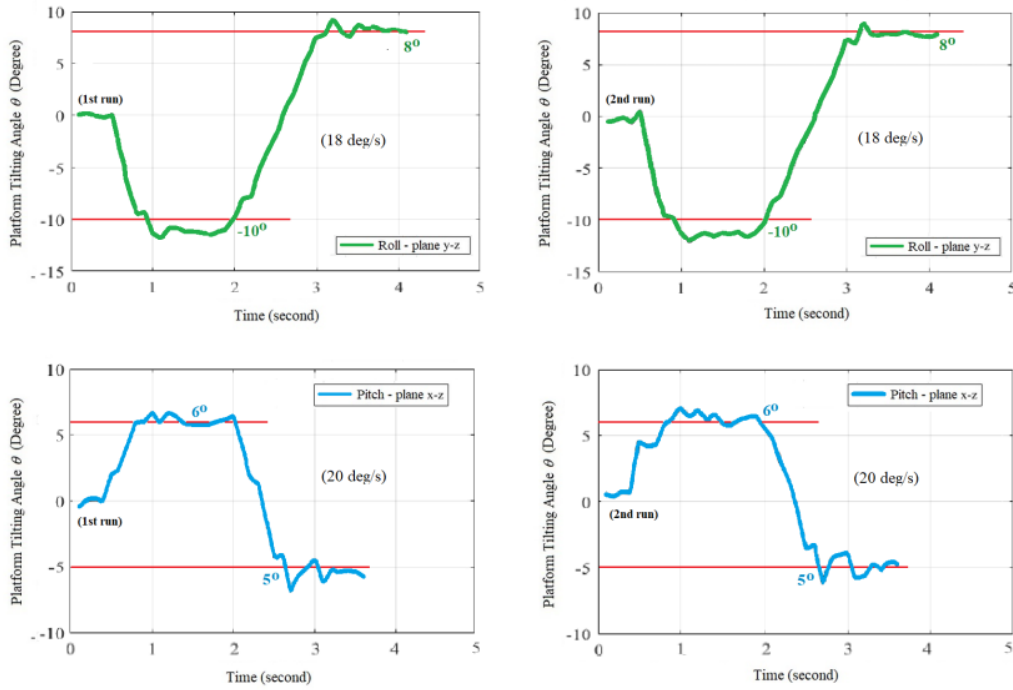


Figure 12. Two running tests from zero to two desired positions

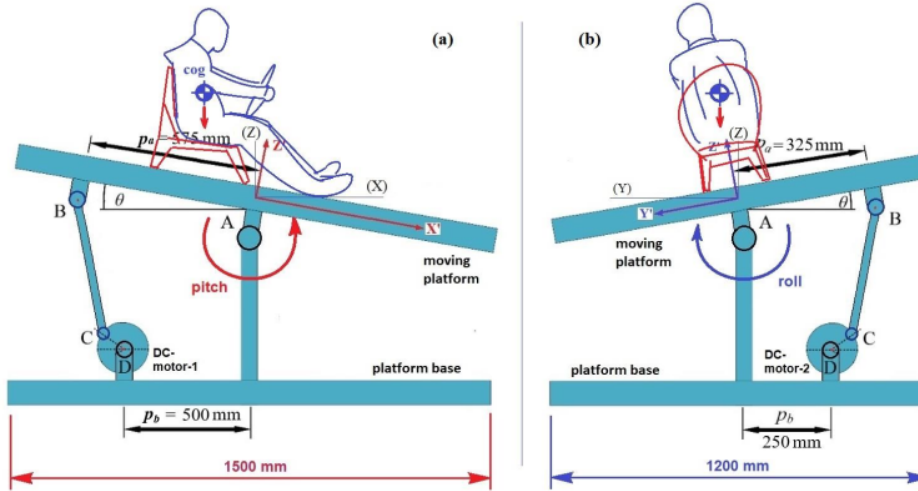


Figure 13. Position of COG which will influence the dynamic effect

dynamic model, the motor torque required to move the platform can be determined more precisely and accurately. This point is the consequence of the COG position concerning the pivot point that alters corresponding to the tilting angle. This phenomenon must be taken care of in developing the motor controller.

#### IV. Conclusion

In this study, the preliminary design of a 2-DOF moving platform has been introduced to demonstrate motions that

might be experienced by the user (car driver) in roll and pitch directions. The limited range of motion is determined to fulfill the rules of the vestibular system, where humans can only sense the tilting angle of 6°. To obey this rule, the first motor angle between -26° and 27° is suitable for the roll plane, while the angles range of -52° and 54° is suitable for the pitch plane. A kinematic model of the platform is developed, and the resulting mathematical expression generates the relation between the driving motor angle and the tilting angle of the platform.



Simulation and experimental results show a good fit between them. This demonstrates that the model is acceptable based on the orientation error on both planes being less than 5%. Four different experiments were carried out to show the ability of this design to move from any pose in the roll and pitch plane to the home position. Depending on the magnitude of the offset, the traveling time still needs to be justified to ensure that it will give the appropriate radial velocity. But from some experiments conducted above, the maximum rotational speed of the platform is 20 deg/s. As mentioned earlier, the acceptable radial velocity of the human vestibular system should not be higher than 3.7 deg/s, as suggested by previous work. It concludes that the speed in those experiments is not suitable for human application, but the objective of this work is not the speed criteria but the degree of orientation. This issue will be dealt with in future work.

## References

- [1] K. A. Brookhuis, "Driving simulator," in *International Encyclopedia of Transportation*, Elsevier, Amsterdam, The Netherlands, pp. 14-19, 2021.
- [2] O. X. Kuiper, J. E. Bos, C. Diels, and K. Cammaerts, "Moving base driving simulators' potential for carsickness research," *Applied Ergonomics*, 81, 102889, pp. 1-5, 2019.
- [3] Y. Maruyama and S. Sakaki, "Development of driving simulator for the experiment of tsunami evacuation using automobile," in *Proc. of the 7th International Conference on Asian and Pacific Coasts (APAC)*, pp. 454-459, 2013.
- [4] A. E. Gomez, T. C. dos Santos, C. M. Massera; A. M. Neto, and D. F. Wolf, "Driving simulator platform for development and evaluation of safety and emergency systems," *Computer Science: Computers and Society*, Cornell University, 2018.
- [5] A. Berthoz, W. Bles, H. Bühlhoff, B. C. Grácio, P. Feenstra, N. Filliard, R. Hühne, A. Kemeny, M. Mayrhofer, M. Mulder, H. Nusseck, P. Pretto, G. Raymond, R. Schlüsselberger, J. Schwandtner, H. Teufel, B. Vaillieu, M. M. Van Paassen, M. Vidal, and M. Wentink, "Motion scaling for high-performance driving simulators," in *IEEE Transactions on Human-Machine Systems*, 43 (3), pp. 265-276, 2013.
- [6] S. Khan and R. Chang, "Anatomy of the vestibular system: a review," in *Neuro Rehabilitation*, vol. 05, no. 32, pp. 437-443, 2013.
- [7] P. Hansson, A. Stenbeck, A. Kusachov, F. Bruzelius, and B. Augusto, "Prepositioning of driving simulator motion systems," *Int. J. Vehicle Systems Modelling and Testing*, vol. 10, no. 3, pp. 288-304, 2015.
- [8] L. V. Bringoux, L. Marin, P. A. Barraud, and C. Raphel, "Contribution of somesthetic information to the perception of body orientation in the pitch dimension," in *The Quarterly Journal of Experimental Psychology Section A*, vol. 56, no. 5, pp. 909-923, 2003.
- [9] A. Stratulat, V. Roussarie, J. L. Vercher, and C. Bourdin, "Improving the realism in motion-based driving simulators by adapting tilt-translation technique to human perception," in *IEEE Virtual Reality*, pp. 47-50, 2011.
- [10] E. Groen and W. Bles, "How to use body tilt for the simulation of linear self-motion," *Journal of Vestibular Research*, vol. 14, no. 5, pp. 375-385, 2004.
- [11] N. C. Ruiz-Hidalgo, A. Blanco-Ortega, A. Abúndez-Pliego, J. Colín-Ocampo, and M. Arias-Montiel, "Design and control of a novel 3-DOF parallel robot," in *Proc. International Conference on Mechatronics, Electronics and Automotive Engineering*, pp. 66-71, 2016.
- [12] X. Hu, F. Li, and G. Tang, "Kinematics analysis of 3UPU-UP coupling parallel platform in the marine environment," *IEEE Access*, vol. 8, pp. 158142-158151, 2020.
- [13] A. Adel, M. Mahmoud, N. Sayed, O. Hisham, O. Ossama, P. Adel, Y. Ayman, M. I. Awad, Shady A. Maged, S. M. Umer, H. Iqbal, and H. F. Maqbool, "Design of A 6-DOF hydraulic vehicle driving simulator," in *Proc. Int. Conf. on Innovative Trends in Communication and Computer Engineering*, Egypt, pp. 170-175, 2020.
- [14] H. Arioui, S. Hima, L. Nehaoua, R. J. V. Bertin, and S. Espié, "From design to experiments of a 2-DOF vehicle driving simulator," *IEEE Transactions on Vehicular Technology*, 60 (2), pp. 357-368, 2011.
- [15] M. V. K. Reddy, "Orientability of the moving platform in planar cable robots," Master Thesis, Mechanical Engineering, Indian Institute of Science, Bengaluru - 560012, India, 2019.
- [16] J. Tiana-Alsina, M. A. Gutierrez, I. Wurth, J. Puigdefabregas, and F. Rocadenbosch, "Motion compensation study for a floating Doppler wind LIDAR," in *Proc. IEEE International Geoscience and Remote Sensing Symposium (IGARSS)*, pp. 5370-5382, 2015.
- [17] N. Ahmad, M. K. A. Kholdun, H. Zulkefle, M. F. Abdullah, D. Kamaruzzaman, and N. E. Abdullah, "2 degree of freedom (DOF) motor control for motion simulation," in *Proc. IEEE 12th Control and System Graduate Research Colloquium (ICSGRC 2021)*, pp. 259-264, 2021.
- [18] M. N. A. Bin Mohd Nadiman, "Design and development of 2-DOF motion simulator for paramotor trike," Master Thesis, Faculty of Engineering, University of Malaya, 2020.
- [19] H. M. Saputra, Z. Abidin, and E. Rijanto, "IMU application in measurement of vehicle position and orientation for controlling a pan-tilt mechanism," *Journal of Mechatronics, Electrical Power, and Vehicular Technology (MEV)*, 04, (1), pp. 41-50, 2013.
- [20] A. A. Rafiq, W. N. Rohman, and S. D. Riyanto, "Development of a simple and low-cost smartphone gimbal with MPU-6050 sensor," *Journal of Robotics and Control (JRC)*, 1(4), pp. 136-140, 2020.
- [21] Y. Zhang, K. Song, J. Yi, P. Huang, Z. Duan, and Q. Zhao, "Absolute attitude estimation of rigid body on moving platform using only two gyroscopes and relative measurements," *IEEE/ASME Transactions on Mechatronics*, 23, (3), pp. 1350-1361, 2018.
- [22] A. F. Albaghdadi and A. A. Ali, "An optimized complementary filter for an inertial measurement unit contain MPU6050 sensor," *Iraqi Journal for Electrical and Electronic Engineering*, 15, (2), pp. 71-77, 2019.
- [23] A. Jefiza, E. Pramananto, H. Boedionoegroho, and M. H. Purnomo, "Fall detection based on accelerometer and gyroscope using back propagation," in *Proc. EECSEI 2017*, pp. 19-21.
- [24] Z. T. Al-Dahan, N. K. Bachache, and L. N. Bachache, "Design and implementation of fall detection system using MPU6050 Arduino," *Springer International Publishing Switzerland*, pp. 180-187, 2016.
- [25] I. Rifajar and A. Fadlil, "The path direction control system for lanange jagad dance robot using the MPU6050 gyroscope sensor," *International Journal of Robotics and Control*, pp. 27-40, 2021.



1 %

SIMILARITY INDEX

### PRIMARY SOURCES

- 1

deepai.org  
Internet

33 words — 1 %
- 2

Hansson, P., A. Stenbeck, A. Kusachov, F. Bruzelius, and B. Augusto. "Prepositioning of driving simulator motion systems", International Journal of Vehicle Systems Modelling and Testing, 2015.  
Crossref

28 words — < 1 %
- 3

Mohammad Iqbal, Karmilasari, Kemal Ade Sekarwati, Dian Kemala Putri. "Driving Simulator Software for Evaluation of Safety Driving", 2020 Fifth International Conference on Informatics and Computing (ICIC), 2020  
Crossref

8 words — < 1 %
- 4

Mohammad Reza Chalak Qazani, Houshyar Asadi, Chee Peng Lim, Shady Mohamed, Saeid Nahavandi. "Prediction of Motion Simulator Signals Using Time-Series Neural Networks", IEEE Transactions on Aerospace and Electronic Systems, 2021  
Crossref

8 words — < 1 %
- 5

Zoran Vrhovski, Karlo Obrovac, Alan Mutka, Stjepan Bogdan. "Design, modeling and control of a system for dynamic measuring of leg length discrepancy", 2017 21st International Conference on System Theory, Control and Computing (ICSTCC), 2017

8 words — < 1 %

---

EXCLUDE QUOTES	ON	EXCLUDE SOURCES	OFF
EXCLUDE BIBLIOGRAPHY	ON	EXCLUDE MATCHES	OFF